J. Fluid Mech. (1995), *vol.* 300, *pp.* 71–85

Surfactant effects on the dynamics of a thin liquid sheet

By LUIGI DE LUCA[1]† AND CAROSENA MEOLA[2]

[1] Politecnico di Torino, Department of Aerospace Engineering, Corso Duca degli Abruzzi, 24, 10129 Turin, Italy

[2] Università di Napoli, DETEC P.le Tecchio, 80, 80125 Naples, Italy

(Received 4 October 1993 and in revised form 5 May 1995)

The dynamics of a free-surface slender two-dimensional stream (liquid sheet) issuing from a nozzle in the gravitational field in still air, under the effect of surface-active agents, are analysed experimentally. The particular test section geometry (the liquid is forced to assume a bidimensional form between two vertical guides and a horizontal plate placed at a certain variable distance from the nozzle exit section) employed in this study gives rise to various flow regimes depending on the governing parameters: liquid flow rate, sheet height, surface pressure, gravity. Two basic phenomena are observed: thinning of the sheet (with recirculating motion inside it) and sheet–threadlines transition. For a certain surfactant (bulk) concentration, there exists a minimum critical flow rate value for which the sheet is seen to thin starting at both of the sheet bottom corners. A ridge, usually referred to as a *Reynolds ridge* in the literature, separates the sheet from the thin-film regions. The thin films exhibit recirculating flows (caused by the onset of surfactant-induced surface-pressure-driven convection in the gravitational field) and extend to the entire rectangular interface as the flow rate is reduced. At zero flow rate the thinned sheet resembles a plane vertical soap film showing a recirculating cellular structure. These phenomena are linked to the presence of surface-active material adsorbed at the liquid–air interface and occur when the sheet height exceeds a critical value. Otherwise, at a critical flow rate value the liquid sheet breaks up into an array of (more or less regularly distributed) discrete threadlines (vertical jets), whose spacing depends on the surface tension of the test liquid.

1. Introduction

The dynamics of thin sheets of liquid and their disintegration were first studied by Squire (1953) and Taylor (1959). Later, Brown (1961) carried out an experimental investigation on the general behaviour of a liquid sheet in connection with the so-called curtain coating process. He observed that the curtain disintegrated if the liquid flow rate was reduced to a certain minimum value. Brown's finding was confirmed experimentally by Lin & Roberts (1981) and theoretically by Lin (1981) who used linear stability analysis. On the other hand, Carlomagno (1974) extended Lee's (1963) work on the instability of a film coating a two-dimensional cylinder to the case of a continuous downflow from the cylinder. Basically depending on the flow rate value, different flow regimes were observed: sheets, sheets and discrete vertical jets (or threadlines), jets, drops. In particular, the position of threadlines was thought to coincide with the spots of droplets observed by Lee (1963) and Carlomagno (1974) himself in the *static* situation, i.e. without a continuous liquid supply. Flow regimes

† Present address: Università di Napoli, DETEC P.le Tecchio, 80, 80125 Naples, Italy.

qualitatively similar to those above mentioned were found by Pritchard (1986), who studied the free-surface class of flows arising when the fluid (a commercial vegetable oil) is poured over the end of a flat plate into a reservoir well below the plate. This class of flows was found to be highly unstable with over seven hundred different flow regimes observed in the experiments, some of which were steady and some nearly periodic in time exhibiting a less regular, almost chaotic behaviour in time. More recently, the regimes described above have also been observed by Limat *et al.* (1992) in an experimental set-up similar to that employed by Lee (1963) and Carlomagno (1974), although there is no mention of the two last investigators in Limat *et al.* A horizontal hollow half-cylinder was supplied with liquid (a silicon oil) that overflowed, ran over the external sides and was collected below the cylinder. Depending on the flow rate, the resulting layer (or sheet) might break up either into drops or jets or both. An interesting finding of Limat *et al.* has been that the arrays of drops and/or vertical jets exhibit spatio-temporal phase dynamics: oscillations, pairing or nucleation of cells and forced *tilt waves*.

The present study is concerned with the continuous downflow of a liquid from a nozzle, having a horizontal exit section, in the gravitational field in still air, and is aimed at gaining some insights into the behaviour of the class of flows described above. In fact, as in the observations of Pritchard (1986) and Limat *et al.* (1992), irregular or regular sheets, arrays of vertical jets and drops flow regimes are observed (Carlomagno & de Luca tested this geometry early in 1987) together with a phenomenon that is believed to be a peculiarity of the presence of surfactants in the test liquid, i.e. sheet thinning which is observed to start at the sheet bottom corners. As will be seen later, the formation of thin films may be related to the onset of a locally *clogged* flow, where, following Harper (1992), the word *clogged* is used to mean 'covered with enough surfactant to prevent tangential motion'. In these flows the effects of surface-active agents that are adsorbed at the liquid–air interface are usually quantified in terms of surface pressure (which is a function of the so-called surfactant surface excess) rather than the standard surface tension coefficient.

Depending on the main flow rate, the sheet partially or totally resembles a plane vertical soap film exhibiting recirculating structures inside it. Previous studies on surface-tension-driven flows in thin films were made by Pearson (1958), Levich (1962) and Yih (1968). Later McTaggart (1983) generalized the linear stability analysis of Pearson (for Marangoni instability) to the case where surface tension depends on both temperature and solute concentration. The surfactant-induced surface tension gradients driving convection within a thin film in the gravitational field and causing the (soluble) surfactant to spread, were numerically simulated by Halpern & Grotberg (1992). Koschmieder & Prahl (1990) carried out tests to determine the onset of surface-tension-driven convection as well as the resulting cellular configuration in small containers of different geometry. In particular, the above-cited authors visualized different cellular flow patterns induced by temperature-dependent surface tension variations. Recently, Ji & Setterwall (1994) studied the effect of surface-active solute on the stability of a liquid film flowing down a vertical plane. While the surface-tension-driven (Marangoni) convection has been analysed to a rather large extent, it seems that the formation of thin films with the associated recirculating flow pattern in a freely falling liquid sheet has not been considered. In the present investigation the system is practically isothermal, but the influence of surface-active agents together with possible temperature cross-effects will also be discussed.

Regarding the sheet breakup (leading to the sheet–jets transition), in the authors' opinion the results of the present paper can be taken as a development of those of

Pritchard (1986) and Limat *et al.* (1992) since the surface tension is now varied by adding surface-active agents to water. As far as the conditions for the sheet disintegration are concerned, the criterion proposed by Brown (1961), and recovered by Lin (1981) for a thin liquid curtain, does not include the interfacial adsorption of surfactants. Later, Lin, Lian & Creighton (1990) extended the criterion to take into account the presence of ambient gas. To include the interfacial adsorption of surfactants, Brown's reasoning will be extended to the present situation by considering the surface pressure instead of the surface tension.

2. Experimental apparatus and testing procedure

The experimental apparatus is sketched in figure 1. The test liquid from a tank goes through a regulating valve, a flow rate meter, a flexible tube, a stagnation chamber and is spread out by means of a replaceable stainless steel nozzle, having a horizontal exit section. In order to make the entering liquid uniform a perforated plate (with holes drilled at prefixed points) is placed in the stagnation chamber at about 1/3 of its height. Particular care is taken to eliminate any vibration source, control the ambient air to be quite still, bleed the stagnation chamber, eliminate impurity from the test liquid, and ensure the levelling of the nozzle exit section.

Three nozzle shapes having different lengths L and discharge widths δ_0 are employed, which in the following will be simply referred to as nozzle a, nozzle b, and nozzle c. The cross-section of each of them is shown in figure 1. The values of L and δ_0 are 180 mm and 2 mm respectively for nozzle a and 140 mm and 1 mm for nozzle b. The third nozzle is 275 mm in length and its variable discharge width is taken equal to 1 mm or 2 mm.

Two vertical Plexiglas plates, placed at each end of the nozzle (lateral end plates), facilitate the initial formation of the liquid sheet and allow a simulation of the two-dimensionality of motion. In fact, gravity effects tend to contract the bottom of the sheet, giving it a characteristic triangular shape. A horizontal plate running across the lateral plates is used to fix the height of the liquid sheet (bottom end plate). The liquid is collected in a reservoir below the test section and then pumped back to the tank.

Tests are carried out for (bulk) surface tension σ of the test liquid ranging from 25 to 93.2 dyn cm^{-1}. Note that high values of σ are critical in obtaining an initially stable sheet. This range of surface tension values is achieved by adding either sodium sulphate or surface-active agents to bi-distilled water. The surface tension of such solutions is measured by means of a stalagmometer; the liquid density ρ and the kinematic viscosity coefficient ν are also measured: ρ ranges from 0.997 to 1.096 g cm^{-3} and ν ranges from 0.86 to 1.04 cSt. In order to analyse the role played by the surface-active agents, some tests are performed with vegetable oil without surface-active constituents ($\rho = 0.907$ g cm^{-3}, $\nu = 67.5$ cSt and $\sigma = 34$ dyn cm^{-1}). However, as discussed in the introduction, within the dynamics of the flows studied in the present context, the effects of surface-active agents are better quantified in terms of surface pressure Π, which is defined as

$$\Pi = \sigma_s - \sigma, \tag{1}$$

where σ_s is the surface tension of the solvent (i.e. the pure liquid, water in the present case) and σ is the surface tension of the solution. In effect, if the surface tension of a liquid is lowered by the addition of a solute, then, by the Gibbs model, the solute is adsorbed at the interface. This may amount to enough to correspond to a monomolecular layer of solute on the surface and such a monolayer may be considered to

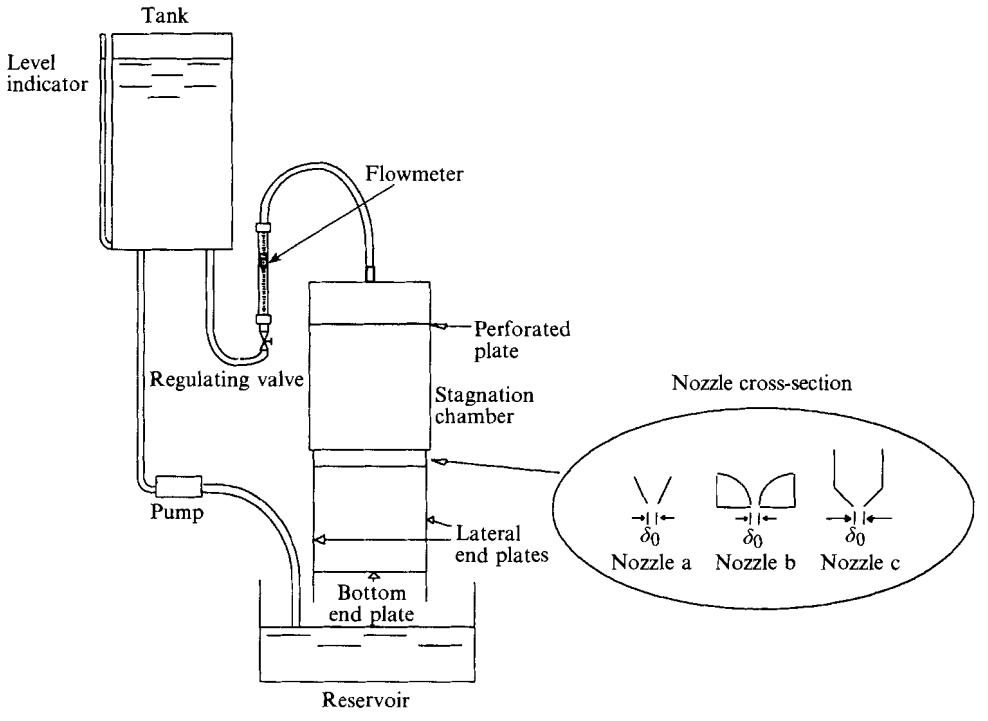

FIGURE 1. Experimental set-up.

exert a film pressure, or surface pressure, Π (Rosen 1989). For dilute solutions the film of adsorbed solute may be supposed to be in a gaseous state and obey to the equation of state of a two-dimensional ideal gas, $\Pi = \Gamma RT$, where Γ is the surface excess concentration (in practice, the surface concentration), R the gas constant, T the absolute temperature. The experimental data will be analysed by taking into account the surface pressure Π evaluated by means of (1).

The vertical position of the bottom end plate z, as measured from the nozzle edge, varies from very small values (generally a few centimetres for high values of σ) to approximately 60 cm (for small values of σ).

In general, the investigations are concerned with observations of the liquid downflow behaviour by variation of the surfactant concentration (i.e. surface tension or surface pressure), the position of the bottom end plate and the flow rate. To better clarify this, experiments, for a certain water solution, generally start with the bottom end plate set at a position relatively close to the nozzle exit section (i.e. a small z value is set). The regulating valve is then opened and set at a value of volumetric flow rate per unit length Q to obtain a stable regular liquid sheet bounded by the two lateral plates and the bottom one. Using the valve, the flow rate is decreased slowly to give different flow regimes which are photographed and later analysed. This procedure is repeated for increasing z values until it is no longer possible to create an initial regular two-dimensional sheet (given a certain water solution, for relatively high z values the liquid is unable to follow the lateral plates and assumes a triangular shape). The concentration of surfactants is then varied and the entire procedure is repeated.

3. Qualitative description of flow regimes

At the beginning, when the regulating valve is completely open, the flow is irregular and resembles a waterfall as shown in figure 2. (All the photographs shown hereafter are for nozzle c with $\delta_0 = 1$ mm and a surface tension value of 60 dyn cm^{-1}, that is $\Pi = 15$ dyn cm^{-1}). In this picture, besides the nozzle at the top and the two lateral vertical plates, the bottom plate is also clearly visible under which the waterfall contracts and assumes a characteristic triangular shape. On the other hand, within the rectangular frame bounded by the nozzle exit section, the lateral plates and the bottom one, the liquid is well attached, forming basically a two-dimensional downflow. However, some non-uniformities or corrugations are present especially at the edges of the flow. As the flow rate is decreased the sheet thickness also decreases to reach a thinner, more regular or stable sheet configuration (figure 3).

A further reduction of flow rate gives rise to a particular phenomenon, here called sheet thinning and consisting of the formation of thin films, which start from both of the sheet bottom corners and seem to be related to the aforementioned edge effects. The thin-film regions are characterized by no mean flow rate, apart from a recirculating flow inside them, and are separated from the flowing thicker sheet by a ridge visible in both of the bottom corners of figure 4. The separating ridges generally exhibit a time-fluctuating behaviour, which can interfere with the recirculating structure developed in the thinned zones. Such ridges are believed to be what in literature is generally referred to as a *Reynolds ridge* (Scott 1982; Harper 1992), which is described as a local slight rise in the surface level of a flowing liquid at the transition from a free surface (shear stress negligible) to a clogged surface (surface velocity negligible) where the tangential gradients of the surface concentration of surfactants (linked to the surface pressure) create shear sufficient to oppose surface motion. What is described above is the typical situation of a stream flowing against an obstacle, such as the horizontal plate of the present experiments. The surfactants, generally, accumulate upstream of the obstacle; thus, the liquid, flowing towards the obstacle, encounters the leading edge of a stagnant, almost incompressible layer of surfactants and is forced below it, forming a viscous boundary layer. Another physical application of clogged flows is the so-called stagnant cap which may form on a bubble or drop moving steadily in a liquid (Lerner & Harper 1991).

The presence of the Reynolds ridge at the transition to clogged flow is strictly related to the diffusion of surface-active material to free surfaces of the liquid, where it reduces the surface tension and gives the surface elastic properties to resist compression. It is expected that only as surfactant fully diffuses to the surface is the equilibrium value of its surface concentration (i.e. of the surface pressure Π) reached. As an opposite limiting case, a freshly created surface has a value of Π near zero. In the present experiments the attainment of the conditions for thinning onset may be verified by comparing the diffusion time scale for the surfactant to the typical time of descent of the water solution. The former may be estimated as δ^2/D, where δ is the local sheet thickness and D is the surface diffusivity of adsorbed surfactants. The classic inviscid inertia–gravity model applied to vertically falling sheets gives $(2z/g)^{1/2}$, where z is the sheet height and g the gravity acceleration (it is believed that viscosity does not play a key role in the present observations). Harper (1992) indicated that ordinary surfactants on water have $D/\nu = 4 \times 10^{-4}$, where ν is the kinematic viscosity of water and, hence, if $z = 10$ cm and $\delta = 0.1$ mm are assumed as typical values, the diffusion time is about 25 s and the descent time about 0.14 s. Note that the ratio of the diffusion time to the descent time may be also represented by the Péclet number. This parameter,

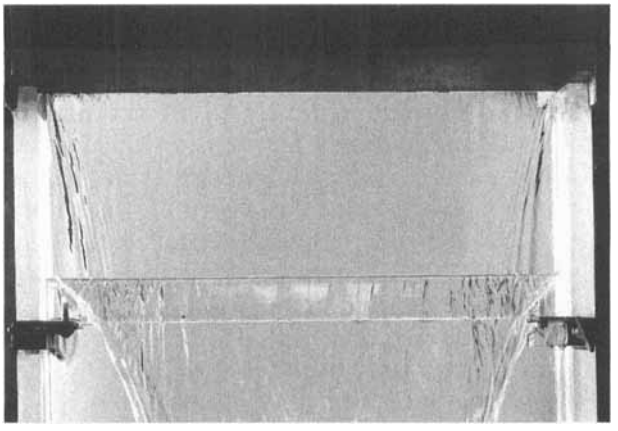

FIGURE 2. Irregular sheet: $z = 10$ cm, $Q = 3.50$ cm^2 s^{-1}.

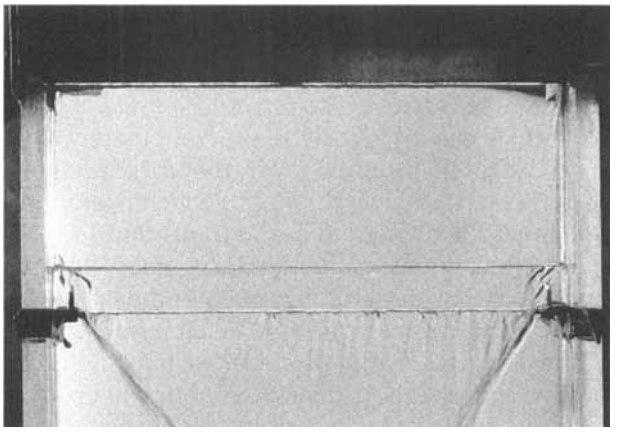

FIGURE 3. Stable sheet: $z = 10$ cm, $Q = 1.75$ cm^2 s^{-1}.

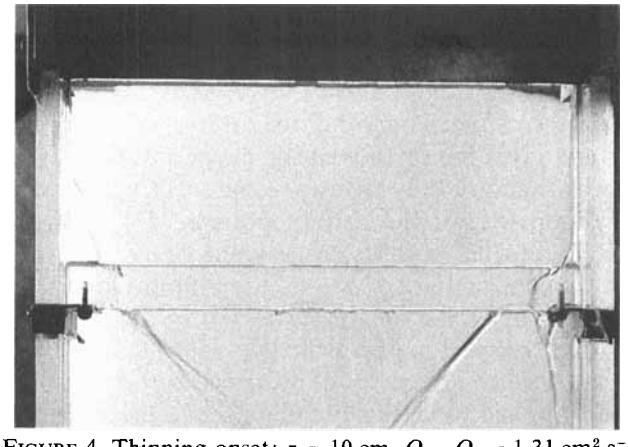

FIGURE 4. Thinning onset: $z = 10$ cm, $Q = Q_c = 1.31$ cm^2 s^{-1}.

in the present context, can be defined as $Pe = Q/D$, which is typically much greater than unity and implies that the lowered surface tension, i.e. higher surface pressure, does not generally apply. However, it has to be noted that the liquid close to the end plates falls down very much slower than that falling freely. Hence, highest surface

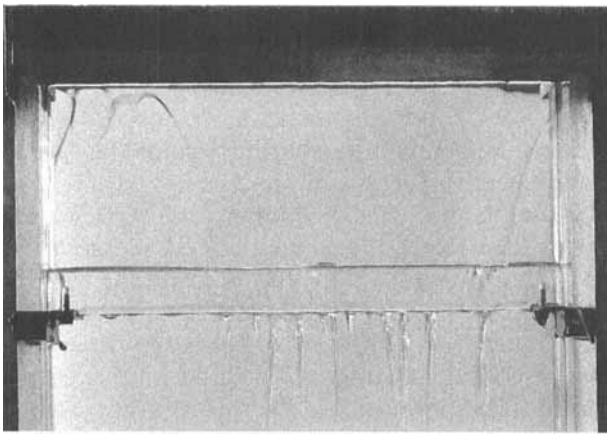

FIGURE 5. Extension of thinning: $z = 10$ cm, $Q = 0.81$ cm^2 s^{-1}.

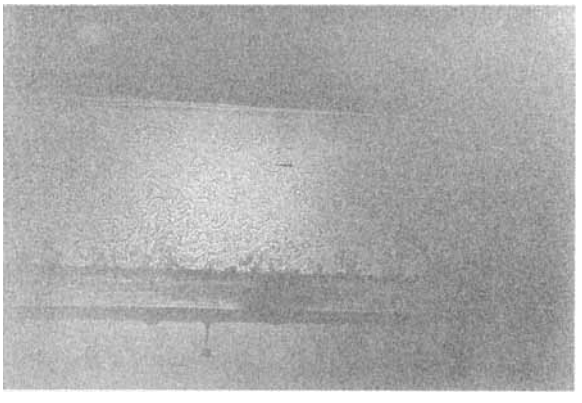

FIGURE 6. Thinned sheet with recirculating cells structure: $Q = 0$ cm^2 s^{-1}.

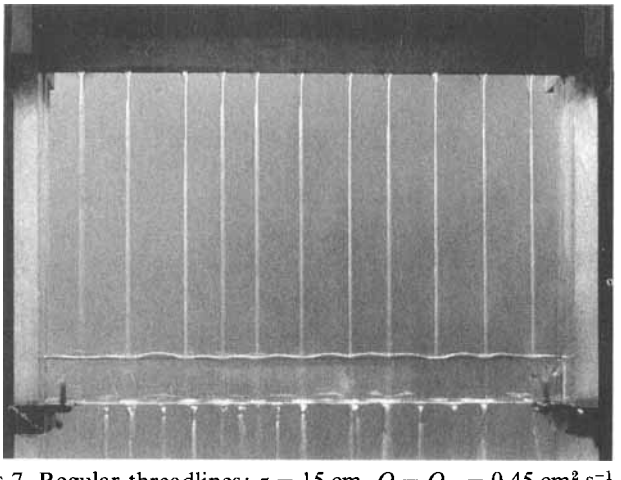

FIGURE 7. Regular threadlines: $z = 15$ cm, $Q = Q_{th} = 0.45$ cm^2 s^{-1}.

pressure values can occur at the sheet bottom corners where there is enough concentration of surfactants to hinder tangential motion. If the falling sheet is thin enough the (creeping) vertical motion between the two liquid–air interfaces, where surfactants collect, is totally choked and the thin film starts to form.

As already mentioned in the introduction, a recirculating flow regime is observed in the thin-film regions. This phenomenon may be explained in terms of film elasticity, Gibbs and Marangoni theories, as described by Rosen (1989) and in a more recent paper by Halpern & Grotberg (1992) on the dynamics and transport modelling of a localized surfactant on a thin film in the gravitational field. It should be noted that film elasticity is possible only if surface-active agents are present. In fact, the tests carried out with vegetable oil do not show the presence of thinning and recirculating flow regimes. In the present experiments the observed recirculating flow pattern is basically due to the variation of the surfactant concentration that is arranged to produce gradients of surface pressure balancing the tangential boundary layer stress. Moreover, in the case of the downflow of aqueous solutions a temperature-dependent surface tension variation might also be considered since a variation of concentration of surfactant could be produced by local evaporation. In other words, the system could be subjected to a surface tension variation associated with a temperature lowering. In the case of evaporation, concentration and temperature effects act in opposite ways because the surface tension decreases with increasing concentration but increases with decreasing temperature.

As the flow rate is further reduced the thinned regions affected by recirculation grow in size and extend to the entire interface. Figure 5 shows a non-symmetric configuration: on the left-hand side, the (irregularly shaped) ridge separating the recirculating flow within the thin film from the main gravitational downflow is very close to the nozzle exit section. At zero flow rate a very thin film (akin to a soap film) is finally created exhibiting the cellular flow pattern shown in the flow visualization of figure 6 obtained by means of a schlieren technique. It is worth noting that the recirculating flow cells configuration, in still air, can maintain its form for hours until an accidental event causes its disintegration.

The formation of the cellular recirculating flow within the thin-film zones occurs provided that the sheet height does not exceed a critical value. Otherwise, at a certain finite value of the flow rate, Q_b, the liquid sheet breaks up giving rise to mixed regimes of either regular or irregular sheets, arrays of vertical jets as well as drops. In this context the most striking result is that regarding the value of the flow rate, Q_{th}, corresponding to the formation of a regular array of vertical jets (or threadlines) at approximately evenly spaced points along the nozzle exit section (figure 7), which is found to be practically constant (i.e. independent of the surface tension). It has also been observed that, owing to some (uncontrolled) circumstances, if the breakup occurs at a flow rate value lower than Q_{th} one or more threadlines is missing, (figure 8), the spacing between them being essentially independent of the flow rate, but dependent on the surface tension alone. This finding is in general agreement with observations of Limat *et al.* (1992). By contrast, if the breakup occurs at a flow rate value greater than Q_{th} the threadlines may be unstable in time and some of them can coalesce as shown in figure 9. It should be remarked that, according to the number of missing jets and their location as well as the number of jets involved in the coalescence process and the number and location of the resulting sheets, a wide variety of (steady and/or time-dependent) situations similar to those of figures 8 and 9 can take place.

The large variety of flows encountered (after breakup) by Pritchard (1986) may be categorized into three main groups corresponding to one of the following situations: uniform distribution, lack or coalescence of jets. Concerning the instability mechanism leading to the sheet breakup, Lin *et al.* (1990) interpreted the sheet disintegration as a capillary rupture, being insensitive to the viscous effects and the gas-to-liquid density ratio. Thus the governing parameter is believed to be the Weber number, which

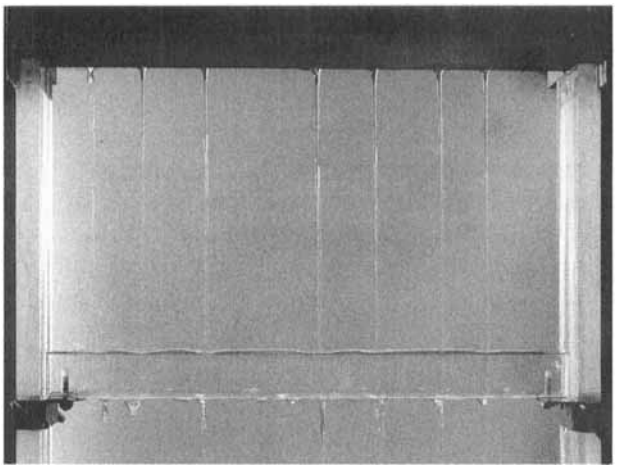

FIGURE 8. One threadline missing: $Q = 0.35\ \text{cm}^2\ \text{s}^{-1}$ ($Q < Q_{th}$).

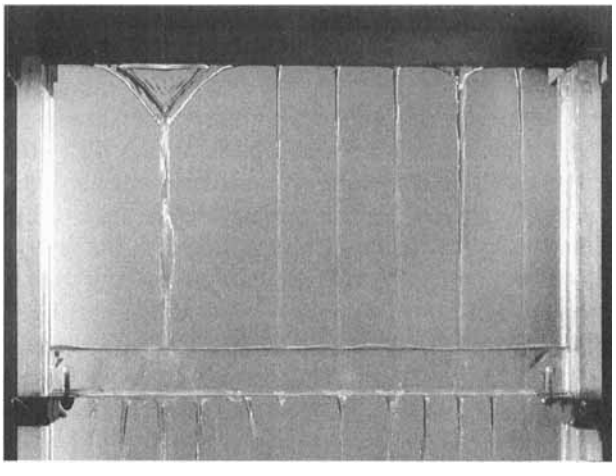

FIGURE 9. Coalescence of threadlines: $Q = 0.70\ \text{cm}^2\ \text{s}^{-1}$ ($Q > Q_{th}$).

measures the relative importance of the inertia forces with respect to the capillary ones. As will be discussed in the next section, the criterion proposed by Brown (1961), and recovered by Lin (1981) for the breakup of a thin liquid curtain, does not consider the interfacial adsorption of surfactants. However, Brown's reasoning may be extended to this last situation by involving the surface pressure instead of the surface tension.

In summary, for each surface tension value, the liquid sheet motion is characterized by two significant values of the flow rate: Q_c, the critical value related to the onset of sheet thinning (or, in other words, the formation of thin films showing recirculating flow); and Q_b, related to the sheet breakup. In addition, two significant values are also found for the sheet height: z_c, the maximum height that enables the entire sheet to be transformed into a recirculating soap film at zero (main) flow rate; and z_{max}, the maximum value that allows the formation of an initial regular two-dimensional liquid sheet. Thus, the variation of Q and z leads to the following behaviour.

(i) For $z \leqslant z_c$ and $Q = Q_c$ the sheet begins to thin at the two bottom corners and the recirculating flow starts; as the flow rate is further reduced the thinned regions grow

in size and extend to the entire interface. At zero flow rate a very thin film, resembling a plane vertical soap film, is finally created.

(ii) For $z_c < z \leqslant z_{max}$ and $Q = Q_c$ the thinning process starts, as described above, but it cannot be completed and when $Q = Q_b$ ($Q_b < Q_c$) the sheet breaks up.

(iii) For $z > z_{max}$ there is a loss of motion two-dimensionality.

The nozzle geometry does not seem to play a key role apart from some drawbacks related to the nozzle discharge width and the extreme values of the surface tension. In fact, when the nozzle width of $\delta_0 = 2$ mm is tested at low values of σ the resulting very thin thickness of the sheet gives rise to the inclusion of air into the nozzle with consequent intermittent spreading out of liquid. On the other hand the nozzle width of $\delta_0 = 1$ mm shows a critical behaviour at high values of σ because, in this case, the sheet thickness or jet diameter exceeds the nozzle width producing a time instability of the threadlines.

4. Quantitative data

It is useful to consider the measured quantities one at a time and to analyse their behaviour under variation of the concentration of surfactants whose effects may be, within the present context, summarized in the surface pressure defined by (1).

The critical flow rate Q_c (thinning onset) trend is plotted in figure 10(*a*) for the three tested nozzles. Apart from the influence of the nozzle discharge section width, it is clearly evident that Q_c increases strongly as the surface pressure increases. On the other hand, as already mentioned, the sheet breakup flow rate Q_{th}, corresponding to the formation of regularly distributed vertical jets, can be considered practically constant (approximately 0.50 cm^2 s^{-1}) to the accuracy feasibility of such difficult measurements.

The variation of the sheet critical height z_c, within which the flow rate can be reduced to zero without sheet breakup, is reported in figure 10(*b*). Since a higher surface pressure corresponds to a wider range of sheet vertical lengths at which the sheet itself is stable, it might be argued that from this point of view the surface-active agent effects are stabilizing. In the previous section it has been observed that where the falling sheet is thin enough the (creeping) vertical motion between the two almost stagnant liquid–air boundaries, where surfactants collect upstream of the horizontal plate, is totally choked and thin films can be formed. It may be expected that at thinning onset the gravitational force effect is small compared to that of the capillary forces; actually the Bond number defined as $Bo = \rho g \delta_c^2 / \Pi$ is generally of $O(10^{-3})$, where δ_c is the sheet thickness at $z = z_c$. If the liquid velocity at the nozzle exit section, V_0, is much less than the Torricellian velocity $(2gz)^{1/2}$, the sheet thickness may be evaluated as

$$\delta = Q/(2gz)^{1/2}. \tag{2}$$

The shape of a two-dimensional liquid sheet under the influence of gravity has been studied in several previous works. Among others, Brown (1961) analytically corrected the inviscid inertia–gravity solution to take into account viscous effects. Recently, de Luca & Costa (1995) numerically computed the free-interface shape with inertia, gravity, viscous, surface tension effects all included. It is clearly evident that, for the sheet flow regimes studied in the present paper and for the relatively large z_c, the interface profile of the sheet very closely agrees with that arising from the very simple inviscid inertia–gravity model, (2). In the present tests the Reynolds number (based on the average inlet velocity and the nozzle width) ranges from about 50 to 400, the Stokes number from 40 to 500 and the capillary number from 10^{-3} to 10^{-2}. The Bond number, based on the sheet thickness δ_c, which is calculated from (2) and is related to z_c and Q_c,

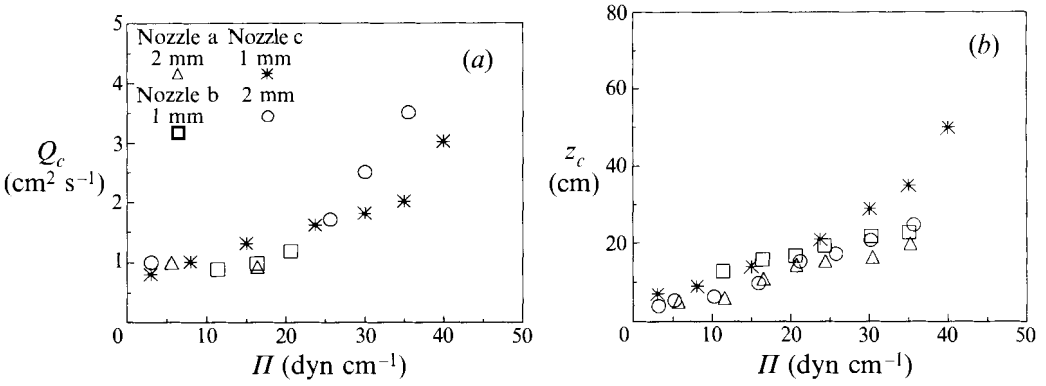

FIGURE 10. Variation of (*a*) the thinning critical flow rate and (*b*) the critical sheet height with surface pressure.

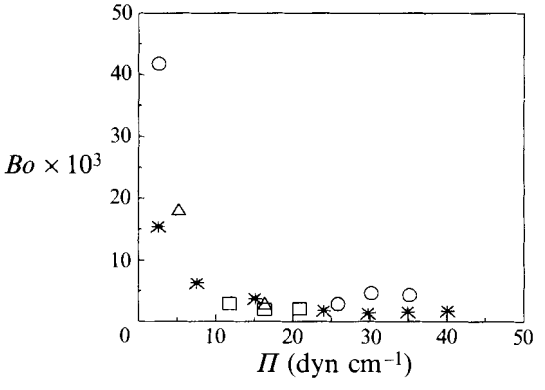

FIGURE 11. Bond number at thinning onset against surface pressure. Symbols as figure 10.

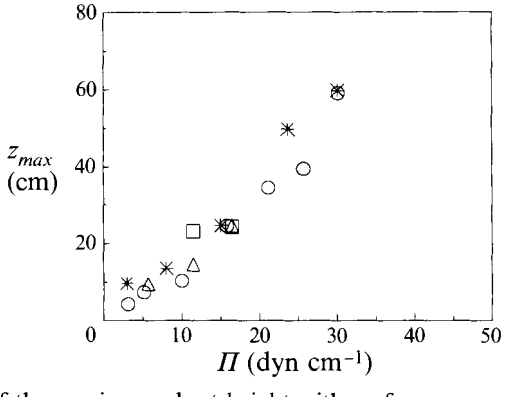

FIGURE 12. Variation of the maximum sheet height with surface pressure. Symbols as figure 10.

is plotted against the surface pressure (i.e. the surfactant surface concentration) in figure 11. For $\Pi > 10$ dyn cm^{-1} Bo is practically constant, while for $\Pi < 10$ dyn cm^{-1} it increases strongly as Π approaches zero. It may be supposed that the first case corresponds to fully clogged flow and the second one to a transitional regime from a free to a clogged surface.

For completeness, the variation of the maximum sheet height z_{max} is reported in figure 12.

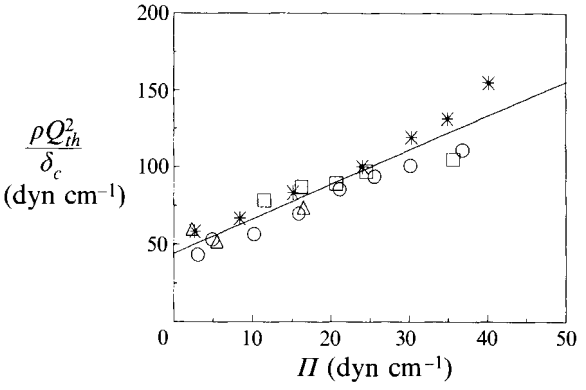

FIGURE 13. Sheet breakup data correlation. Symbols as figure 10.

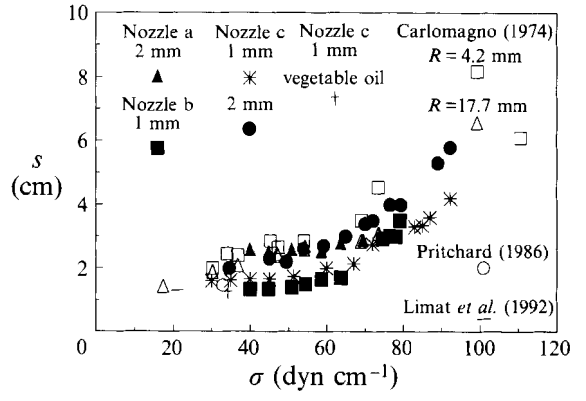

FIGURE 14. Variation of threadline spacing with surface tension.

The instability mechanism leading to the sheet breakup is believed to be a capillary rupture. As pointed out by Brown (1961) and later confirmed experimentally by Lin & Roberts (1981), the sheet disintegration is governed by the (local) Weber number $We = \rho Q^2/\sigma\delta$. Brown observed that at the free edge of a thin sheet equilibrium must be maintained between the surface tension and the inertia forces of the liquid. If a free edge appears because of the formation of a hole in the sheet, then if the momentum flux $\rho V^2\delta = \rho Q^2/\delta$ is greater than 2σ such a hole will not grow, whereas if $\rho Q^2/\delta < 2\sigma$ it will grow and cause the sheet to disintegrate. Thus, if $We > 2$ the sheet is stable. In the present investigation it may be hypothesized that instead of 2σ being the critical value resisting the oncoming momentum it is the surface pressure 2Π. The values of the oncoming momentum $\rho Q_{th}^2/\delta_c$ evaluated at the sheet breakup leading to the formation of jets are plotted against the surface pressure Π in figure 13, where a linear correlation between the two measured quantities may be seen. Again δ_c is evaluated by means of (2) and is related to z_c and Q_{th}. Of course, for a more accurate balance between the two forces, the angle to the vertical, say ϑ, of the ridge separating the thin film and the falling sheet should be considered. In this case the actual component of momentum flux, balanced by Π, is $(\rho Q_{th}^2/\delta)\sin\vartheta$.

In figure 14 the measured (average) threadline spacings s for all the tested nozzle geometries are compared with data available in the literature (only the regimes exhibiting a steady-state behaviour are considered here). Note that the spacing data are reported with respect to the surface tension coefficient σ because the adsorption

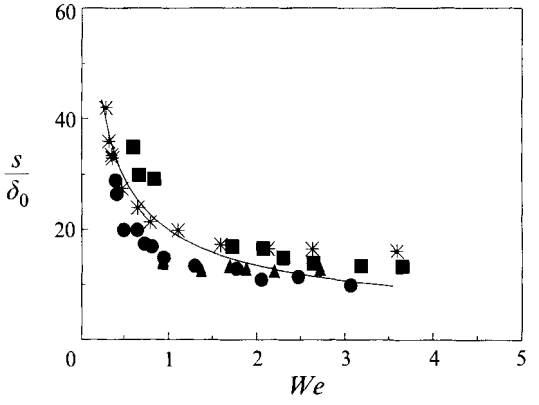

FIGURE 15. Normalized threadline spacing against the local Weber number. Symbols as figure 14.

mechanism of surfactant material at the liquid–air interface is not important in the jet regime. Surprisingly, data points for the case of a continuous supply of fresh liquid, when a nozzle having a discharge width of 2 mm is employed, practically coincide with those obtained by Carlomagno (1974) in the static case. Experiments of Pritchard (1986) and Limat *et al.* (1992) refer to surface tension values of 33 and 21 dyn cm^{-1} respectively and so only two values are reported. The point for vegetable oil practically coincides with that for Pritchard's (1986) experiments.

Furthermore, it can be hypothesized that there exists a correspondence between the observed dimensionless distance between threadlines (the natural choice is s/δ_0) and the appropriate local Weber number $We = \rho Q^2/\sigma\delta$; s/δ_0 is plotted against We in figure 15, where the Weber number is based on Q_{th} and the sheet thickness δ_c. The data points fit the correlation curve shown on the figure

$$s/\delta_0 = 20We^{-0.52} \tag{3}$$

within an acceptable experimental spread.

5. Conclusions

The present experimental work has been aimed at investigating some aspects of the dynamics of a free-surface two-dimensional liquid sheet issuing from a nozzle with a horizontal exit section, in an attempt to gain some insight into the observed interfacial phenomena. In particular, the effects of surface-active agents present in the test liquid have been analysed systematically. Such effects have been quantified in terms of surface pressure (which is a function of the so-called surfactant surface excess) rather than the standard surface tension coefficient.

The particular test section geometry (the liquid is forced to assume a bidimensional form between two vertical guides and a horizontal plate placed at a certain variable distance from the nozzle exit section) employed in this study allowed analysis of various flow regimes depending on the governing parameters: liquid flow rate, sheet height, surface pressure, gravity. Two basic phenomena have been observed: thinning of the sheet (i.e. formation of thin films in some regions of the sheet, exhibiting recirculating motion) and sheet–threadlines transition.

The sheet thinning starts, for a particular flow rate value, at the sheet bottom corners and extends to the entire interface as the flow rate is reduced. At zero flow rate the completely thinned sheet resembles a plane vertical soap film which exhibits a cellular-

type-structure motion. The formation of thin-film zones is believed to be closely connected to the presence of surface-active material in the liquid: in fact, the surfactants, adsorbed at the liquid–air interface, concentrate upstream of the horizontal plate where they form an almost incompressible surface layer. The leading edge of such an incompressible boundary corresponds to the observed local distortion of the interface (generally referred to as a Reynolds ridge), which forces the flowing liquid below it into a boundary layer region. In effect, for the typical flow conditions of the present experiments the Péclet number is much greater than unity, i.e. the descent time of liquid is much shorter than the diffusion time of surfactants. However, close to the lateral plates the liquid velocity is much slower than that of the sheet falling freely and this may explain why the sheet thinning is observed to start at the sheet bottom corners. If the falling sheet is thin enough the vertical motion between the two liquid–air stagnant boundaries, where surfactants collect, is totally choked and allows the thin films to be formed. The Bond number, evaluated at the thinning onset, seems to be constant for fully clogged regimes.

The recirculating flow regime inside the thin films has been hypothesized to be caused by the onset of surfactant-induced surface-pressure-gradient-driven (Marangoni) convection in the presence of the gravitational field. The experimental tests demonstrate the key role played by the surfactants since neither thinning nor recirculating flow is found in the downflow of a vegetable oil. While Marangoni convection has been analysed to a rather large extent in literature, the formation of thin films with the associated recirculating flow pattern in a freely falling liquid sheet has not been considered before.

The aforementioned phenomena are observed to occur provided the sheet does not exceed a certain height (variabling with the surfactants concentration). Otherwise, at a finite flow rate value, the sheet breaks up into discrete threadlines or vertical jets which are approximately equally spaced along the nozzle length, their spacing being basically dependent on the surface tension. A major finding is that the location of the discrete jets is very close to the sites of drops observed in the absence of a continuous liquid supply. There is mention in the literature of similar observations made on different geometries and classified into a large number of spatially and/or temporally unstable flow regimes. In the present work the liquid surface tension is varied (by adding either sodium sulphate or surfactants to water) and the jets spacing is correlated with the Weber number. Only data relative to the regimes exhibiting a steady-state behaviour are included, but an interpretation of the occurrence of some other regimes observed by previous investigators is proposed.

The instability mechanism leading to the sheet breakup is generally interpreted as a capillary rupture (Brown's criterion). To take into account the interfacial adsorption of surfactants, Brown's reasoning has been extended to the present situation by considering the surface pressure instead of the surface tension and it has been found that, at sheet breakup, the oncoming momentum flux is linearly correlated to the surface pressure.

For further insight into the observed phenomena the next step is the development of *ad hoc* models to predict precisely the thinning onset (as well as to simulate the cellular convection) and the sheet–threadlines transition. Other experimental investigations on different geometries (namely nozzle, cylinder, inclined plate) are necessary too.

The authors are greatly indebted to Professor D. H. Peregrine for his helpful comments and suggestions during the revision of the paper.

REFERENCES

BROWN, D. R. 1961 A study of the behaviour of a thin sheet of moving liquid. *J. Fluid Mech.* **10**, 297–305.

CARLOMAGNO, G. M. 1974 Moto di un film liquido su un cilindro orizzontale posto in aria calma. *Proc. II Congr. Naz. AIMETA*, pp. 253–262.

CARLOMAGNO, G. M. & DE LUCA, L. 1987 Instability of a thin liquid sheet in the gravitational field. *Proc. Intl Conf. Fluid Mech., Beijing*, pp. 213–218. Peking University Press.

DE LUCA, L. & COSTA, M. 1995 Two-dimensional flow of a liquid sheet under gravity. *Computers Fluids* **24**, 401–414.

HALPERN, D. & GROTBERG, J. B. 1992 Dynamics and transport of a localized soluble surfactant on a thin film. *J. Fluid Mech.* **237**, 1–11.

HARPER, J. F. 1992 The leading edge of an oil slick, soap film, or bubble stagnant cap in Stokes flow. *J. Fluid Mech.* **237**, 23–32.

JI, W. & SETTERWALL, F. 1994 On the instabilities of vertical falling liquid films in the presence of surface-active solute. *J. Fluid Mech.* **278**, 297–323.

KOSCHMIEDER, E. L. & PRAHL, S. A. 1990 Surface-tension-driven Bénard convection in small containers. *J. Fluid Mech.* **215**, 571–583.

LEE, S. L. 1963 Taylor instability of a liquid film around a long, horizontal, circular cylindrical body in still air. *Trans. ASME* E: *J. Appl. Mech.* **85**, 443–447.

LERNER, L. & HARPER, J. F. 1991 Stokes flow past a pair of stagnant-cap bubbles. *J. Fluid Mech.* **232**, 167–190.

LEVICH, V. G. 1962 *Physicochemical Hydrodynamics.* Prentice Hall.

LIMAT, L., JENFFER, P., DAGENS, B., TOURON, E., FERMIGIER, M. & WESFREID, J. E. 1992 Gravitational instabilities of thin liquid layers: dynamics of pattern selection. *Physica* D **61**, 166–182.

LIN, S. P. 1981 Stability of a viscous liquid curtain. *J. Fluid Mech.* **104**, 111–118.

LIN, S. P., LIAN, Z. W. & CREIGHTON, B. J. 1990 Absolute and convective instability of a liquid sheet. *J. Fluid Mech.* **220**, 673–689.

LIN, S. P. & ROBERTS, G. 1981 Waves in a viscous liquid curtain. *J. Fluid Mech.* **112**, 443–458.

MCTAGGART, C. L. 1983 Convection driven by concentration- and temperature-dependent surface tension. *J. Fluid Mech.* **134**, 301–310.

PEARSON, J. R. A. 1958 On convection cells induced by surface tension. *J. Fluid Mech.* **4**, 489–500.

PRITCHARD, W. G. 1986 Instability and chaotic behaviour in a free-surface flow. *J. Fluid Mech.* **165**, 1–60.

ROSEN, M. J. 1989 *Surfactants and Interfacial Phenomena.* John Wiley & Sons.

SCOTT, J. C. 1982 Flow beneath a stagnant film on water: the Reynolds ridge. *J. Fluid Mech.* **116**, 283–296.

SQUIRE, H. B. 1953 Investigation of the instability of a moving liquid film. *Brit. J. Appl. Phys.* **4**, 167–169.

TAYLOR, G. I. 1959 The dynamics of thin sheets of fluid – III. Disintegration of fluid sheets. *Proc. R. Soc. Lond.* A **253**, 313–321.

YIH, C.-S. 1968 Fluid motion induced by surface-tension variation. *Phys. Fluids* **11**, 477–480.